Boron Removal from Silicon by $CaO-Na_2O-SiO_2$ Ternary Slag

JAFAR SAFARIAN, GABRIELLA TRANELL, and MERETE TANGSTAD

Boron removal from silicon is an important issue for solar-grade silicon feedstock production. In the present study, the removal of B from liquid silicon by a $CaO-Na_2O-SiO_2$ slag is studied and it is shown that B can be rapidly removed from silicon within short refining times. Based on mass balance and chemical analysis of the reacted silicon and slag, it is indicated that the kinetics of B removal is dependent on the Na_2O in the slag, the main reactive agent for B removal from the system. The transported B into the slag is gasified at the slag-gas interface through sodium metaborate evaporation, which is a rate controlling reaction for B transport to the gas phase. It is indicated that B removal rate by $CaO-Na_2O-SiO_2$ slag is considerably higher than that by $CaO-SiO_2$ slags. It is proposed that boron oxide (B_2O_3) is better embedded in the structure of $CaO-SiO_2$ slags than Na_2O-containing slags.

DOI: 10.1007/s40553-015-0048-7
© ASM International (ASM) and The Minerals, Metals & Materials Society (TMS) 2015

I. BACKGROUND

SILICON is the main element used for the fabrication of solar cells and with regard to the renewable energy development it will continue to be a main material in photovoltaic (PV) industry. The production of solar-grade silicon (SoG-Si) through a metallurgical route will be more economic than using the chemical route for silicon production through conventional and modified Siemens process. Directional solidification is an unavoidable refining step for SoG-Si production through any integrated metallurgical route to eliminate many impurities. However, the removal of B and P impurities by directional solidification is not feasible due to their low segregations during silicon solidification. Therefore, employing dedicated refining processes for the removal of B and P from silicon is necessary. Slag refining technique can be considered as a process in which the dissolved B in molten silicon can be removed to low levels required for SoG-Si feedstock *i.e.*, below 1 ppmw, and it is applied currently in industrial scale by ELKEM AS.[1]

The application of various slag systems for B removal from silicon has been recently reviewed by the authors.[2] In general, when slag refining is applied, the dissolved B in silicon melt is partly transferred to the slag phase. The potential of slag for B removal is in principle evaluated by a thermodynamic parameter called distribution coefficient (L_B) and it is the ratio of the concentration of B in the slag over that in silicon. Although higher L_B value shows better B removal from thermodynamic point of view, the kinetics of B removal has to be taken into account, which is affected by the physico-chemical properties of both silicon and slag temperatures and process characteristics. The recent study by authors on B removal using Na_2O-SiO_2 slags[2] indicated that this type of slag may remove B rapidly. In addition, it was shown that parts of the transferred B to the slag reacts with Na_2O and forms sodium metaborate ($Na_2B_2O_4$), which is volatile compared to the slag components and is evaporated at the slag-gas interface.

In the present study, the removal of B from a low Na_2O-containing calcium silicate slag is experimentally studied. The main objective is investigating the effect of Na_2O in the slag on B removal and its comparison with $CaO-SiO_2$ slags[3–9] and $Na_2O-CaO-SiO_2$ slags.[10] Applying $CaO-SiO_2$ slag compositions A, B, and C shown in the ternary $Na_2O-CaO-SiO_2$ slag system in Figure 1, it was observed that the dissolved B in silicon can be rapidly removed through formation of $Na_2B_2O_4$ gas.[2] In this study, the effect of using low amount of Na_2O in $CaO-Na_2O-SiO_2$ slag, slag D in Figure 1, on kinetics of B removal is studied. This may help us to introduce a solution to the main problem in the slag refining of silicon, which is the kinetics of B removal. The obtained results are used to extract more details about the kinetic and mechanism of B removal from silicon by Na_2O-containing slags. In addition, the behavior of the other elements in silicon and slag and their mass transport is studied.

II. EXPERIMENTAL PROCEDURE

A metallurgical grade silicon containing +99.7 wt pct Si was received from ELKEM AS. A synthetic master slag of 47.5 wt pctCaO-5 wt pctNa_2O-47.5 wt pctSiO_2 was prepared through smelting of CaO and SiO_2 powders in a graphite crucible at 1923 K (1650 °C) and later addition of Na_2CO_3 at lower temperature around 1773 K (1500 °C). The concentrations of the impurities in both silicon and slag were measured by inductively coupled plasma–mass spectroscopy (ICP–

JAFAR SAFARIAN, Researcher (PhD), is with the SINTEF Materials and Chemistry, Alfred Getz Vei 2, 7465 Trondheim, Norway. Contact e-mail: Jafar.Safarian@sintef.no GABRIELLA TRANELL, Associate Professor, and MERETE TANGSTAD, Professor, are with the Department of Materials Science and Engineering, Norwegian University of Science and Technology (NTNU), Alfred Getz Vei 2, 7491 Trondheim, Norway.

Manuscript submitted November 1, 2013.
Article published online March 12, 2015

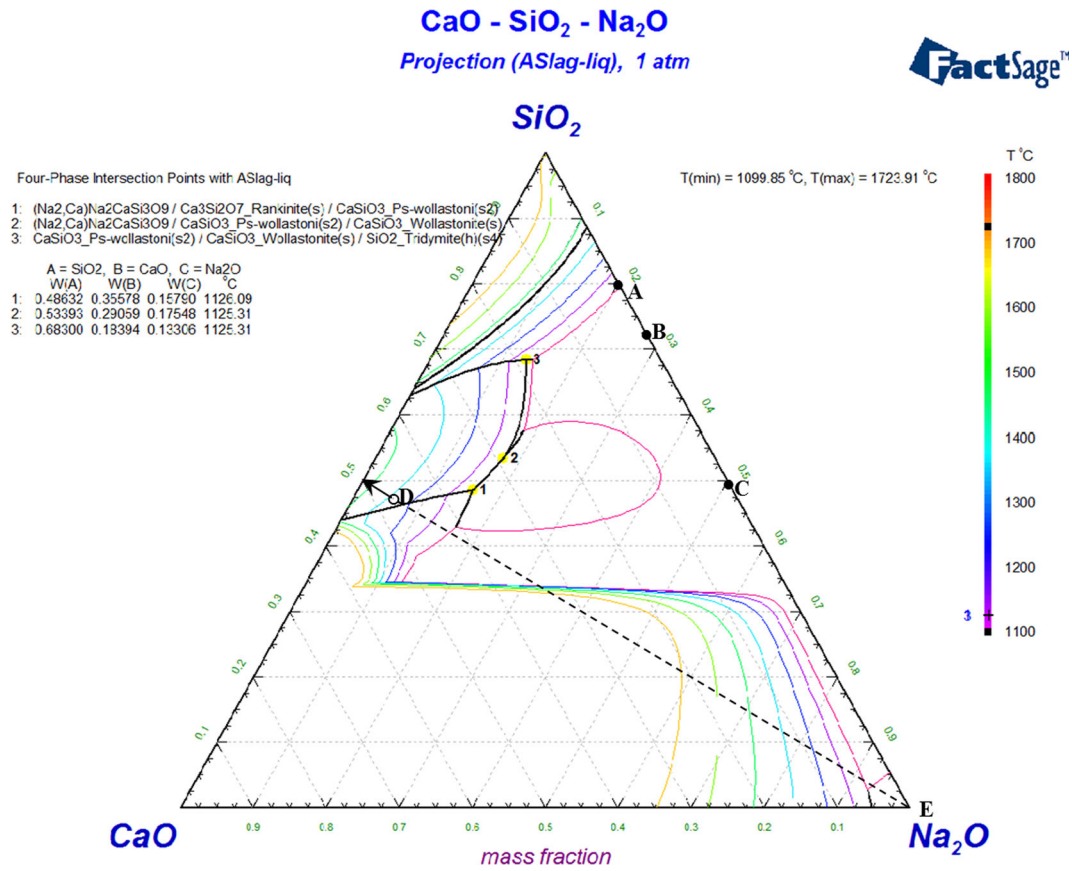

Fig. 1—The ternary phase diagram of CaO-Na_2O-SiO_2 between 1373 K and 1527 K (1100 °C and 1800 °C), calculated by FactSage thermodynamic software version 6.4.

Table I. Chemical Compositions of Silicon and Slag Before Refining Experiments (ppmw)

	B	Ca	Na	Al	Ti	Fe
Silicon	29.81	189.5	—	732.8	15.2	339.8
Slag	0.5	339000	37097	241	1.2	49

MS) and the results are shown in Table I. As seen the B concentration in the slag is low and around 0.5 ppmw, while the silicon contains around 30 ppmw of B.

The slag refining experiments were carried out in an induction furnace containing a water-cooled copper coil (Figure 2). High-purity graphite crucible with 100 mm height, 50 mm outside diameter, and 40 mm inside diameter was used to interact with the silicon and the slag. Around 30 g silicon was put on crucible bottom for each experiment and slag was then charged on top; the slag/silicon mass ratios were 1, 2, and 3 as seen in Table II. The crucible was located in the center of the coil on a quartz support, while surrounded by carbon wool (Figure 2). A thermocouple type C was used to measure the temperature in the melt; it was located in an alumina tube insulator and was put in a graphite thermowell which was fixed in the crucible. The furnace chamber was evacuated two times followed by Ar (+99.999 pct) flashing. Heating was done rapidly under Ar flow to the experimental temperature 1873 ± 5 K (1600 ± 5 °C). According to the ternary phase diagram in Figure 1, the slag is always a liquid single-phase at this temperature and even with possible composition change due to Na_2O reduction. After refining for a period of time (Table II), the crucible was cooled down at a rate around 150 °C/min to below 1273 K (1000 °C). The mass of the crucible before and after the experiments was measured for determining the mass changes through refining as presented in Table II. The reacted silicon and slag phases were carefully separated through cutting the crucibles and separation of silicon and slag. The silicon and slag phases were further crushed and three samples of each one were analyzed by ICP-MS. It is worth mentioning that analysis of silicon and slags by ICP-MS has been done at SINTEF and NTNU for many years and methods for sample preparation, digestion, and analysis have been developed with high level of reliability. In addition, X-ray fluorescence

(XRF) was also used to determine the composition of Na in the reacted slags. It is worth noting that the microstructural analysis of the silicon samples before and after refining may be a useful method to study the purification and the removal of the impurities. However, this method is not beneficial to study B concentration changes in our samples due to very low concentrations of B (less than 30 ppmw), which are much lower than the detection limit of a well-calibrated wavelength-dispersive mass spectrometer (WDS) for B detection in Si matrix, as we experienced to be around 200 ppmw. On the other hand, the segregation coefficient of B between solid and liquid silicon is high and around 0.8,[11] and there is no possibility to see significant B segregation on the grain boundaries. However, ICP analysis techniques are very powerful to analyze many elements in silicon in low concentrations, and they are currently applied in industry.[12]

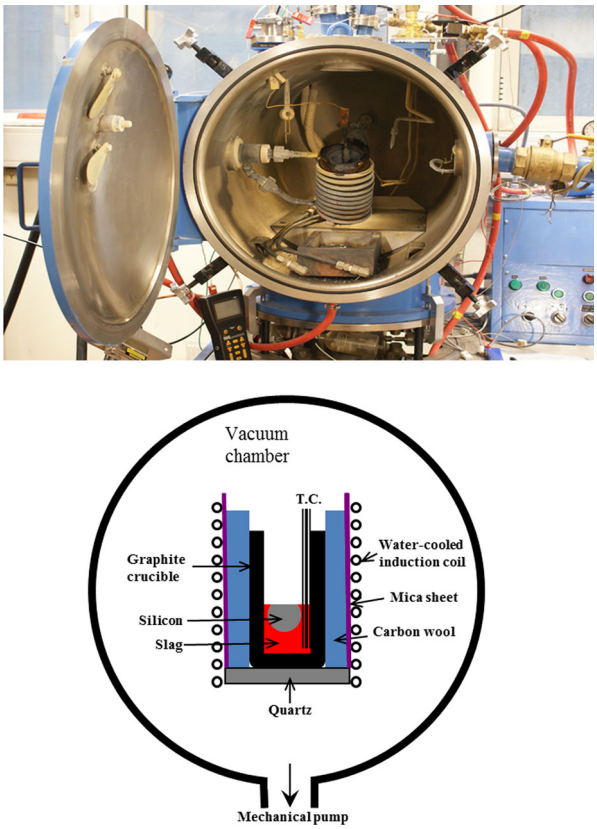

Fig. 2—Induction furnace used for the experiments (*a*) and schematic of the set-up (*b*).

III. RESULTS

The experimental results and observations are described as follows.

A. *Chemical Analyses*

The changes in the chemical compositions of silicon and slag phases during refining are shown in Figure 3. It is observed that the chemical compositions of both slag and silicon are rapidly changed through their interaction and mass transport of B, Na, Ca, and Al takes place during refining. Boron is rapidly removed from the silicon melt and its concentration in silicon is leveled off within short reaction times as clearly seen for the experiments 1 to 4. On the other hand, concentration of B in the slag is rapidly increased and leveled off. Moreover, for a given reaction time, the mass transport of B from silicon to the slag is in larger extent when higher amount of slag is used.

Mass transport of Na from slag to silicon is very fast and Na concentration in silicon reaches a maximum rapidly and then it is decreased with longer refining times as seen in experiments 1 to 4 (slag/silicon = 2). For a given refining time, the concentration of Na in Si is higher when slag/metal ratio is increased as the total input Na in the system is increased. The concentration of Na decreases in all slags over time. This is due to the significant rapid Na loss in the system and its transport to the gas phase. Although the XRF measurements for Na in the slag phase are a little lower than ICP-MS measurements, they support the Na concentration measurements by ICP-MS and the both analysis methods confirm the Na loss from the system.

The presented data in Figure 3 indicate that limited amount of Ca from the slag is transferred to the silicon melt so that the Ca concentration is rapidly increased from 189 ppm to 1000 to 2000 ppm Ca in short reaction time. In contrast, the concentration of Al is rapidly decreased from 733 ppm to below 4 ppm and it is almost completely transferred from the silicon melt to the slag. This shows a high driving force for Al oxidation and its transfer to the slag phase. It is worth mentioning that no significant Fe and Ti transport from the silicon to slag was observed and these elements are mainly staying in the silicon melt.

Table II. Details of the Experiments and Measured Masses Before and After Refining Tests

Experiment	Refining Time (min)	Slag/Metal Ratio	Initial Crucible Mass (g)	Final Crucible Mass (g)	Total Mass Loss (g)	Pct Mass Loss from the Melt
1	10	2	258.34	256.37	1.97	2.19
2	30	2	257.65	255.00	2.65	2.94
3	60	2	257.70	253.84	3.86	4.29
4	120	2	256.47	251.60	4.87	5.41
5	60	1	228.68	226.24	2.44	4.07
6	60	3	288.31	283.38	4.93	4.11

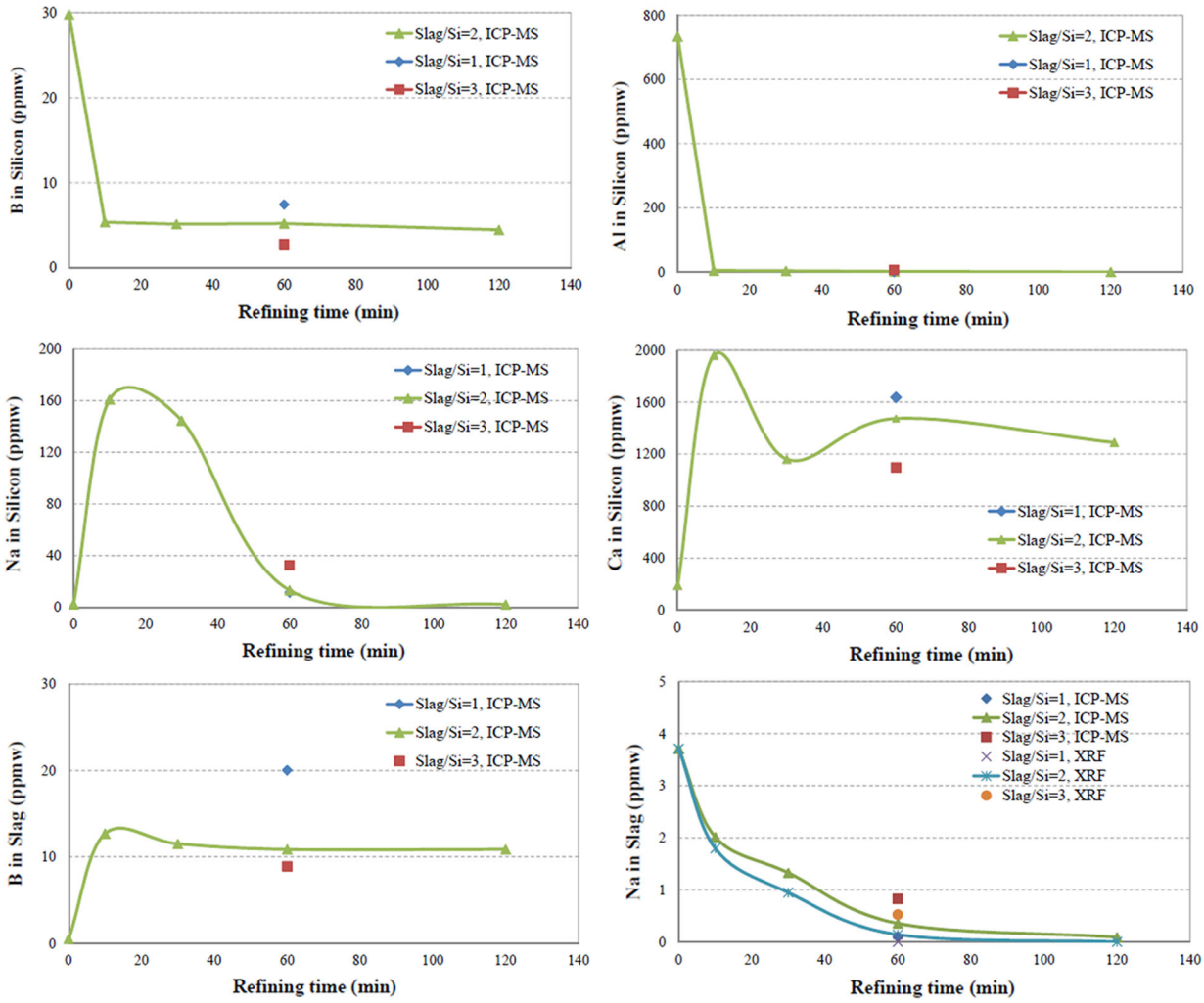

Fig. 3—Chemical composition changes of silicon and slag phases during refining.

B. *Mass Loss*

Measuring the mass of crucibles before and after the experiments indicated significant mass losses as seen in Table II. Obviously, the mass loss is higher for longer refining times, and for a given refining time slightly higher mass losses are observed when larger amounts of slag are used. Assuming negligible mass loss from the graphite, the mass loss percentages from the melts (silicon and slag) can be calculated as presented in Table II. It is seen that when the slag/metal ratio is changed, almost similar mass losses happen within a given refining time. This may indicate that the Na loss, which is the main reason for the mass loss, is taking place with a constant rate and it is not affected by the volume of slag. This may show that the slag-gas and silicon-gas contact areas are not significantly affected by the slag volume change.

C. *Melt Geometry and Phases Contacts*

It was observed that the slag and silicon melts get a geometry in which silicon is like a fluid ball surrounded by the molten slag. Figure 4 shows the cut crucible after two experiments and some silicon samples taken out after the experiments. As clearly seen, silicon does not have any contact with graphite crucible and the graphite thermowell; it is, however, in good contact with the slag and gas phases. Similar melt geometry has been observed for the interaction of Na_2O-SiO_2 slags and silicon in graphite crucible in a resistance furnace,[2] and it was proposed that this melt geometry is due to the lower melting point of the slags compared to silicon and high wettability of graphite by the Na_2O-SiO_2 slags.[2] When the induction furnace is used as this work, the electromagnetic forces may enhance the movement of the slag phase to the crucible walls due to the higher conductivity of the silicon melt than the slag through the mechanism described elsewhere.[13] It is worth mentioning that it was possible to watch the inside of the crucible from the top window of the furnace and a clean and almost flat silicon melt surface was always observed during the experiments.

Fig. 4—Cut crucible showing the melt geometry and the contact of silicon and slag (*a* through *b*), and reacted silicon separated from the slag phase (*c*, *d*, *e*).

D. *Condensate Autoignition in the Furnace*

According to the above chemical analysis and mass losses data, mass transfer from the crucible to the gas phase takes place. The evaporated species are re-condensed on the furnace chamber wall which has low temperature as 293 K (20 °C), since it is cooled by water. This condensate was in contact with Ar during the experiment and when the furnace was cooled down to the room temperature. Autoignition of a thin layer of the condensate over the chamber wall in exposure to the air was observed for all the experiments when the furnace chamber was opened. It is worth noting that the furnace inner wall was cleaned and further washed by ethanol before each experiment.

IV. DISCUSSION

A. *Mass Transport of Elements Between the Phases*

Mass transport of the elements between the silicon, slag and gas phases can be studied through mass balance calculations. The most significant mass changes in the experiments are related to Na_2O depletion from the slag and mass transport to the gas phase. The removed Na from the melts can be calculated by mass balance considering the chemical analysis of the phases and assuming negligible evaporation of the other elements in the melts. The calculated values for Na_2O loss and their comparison with the total measured mass losses in Figure 5 indicate that the main reason for the mass loss is due to Na_2O reduction from the slag along line DF in the shown phase diagram in Figure 1. Considering Na_2O reduction by the graphite wall as the dominant reaction in the system, some carbon is also removed:

$$(Na_2O) + C = 2Na(g) + CO(g). \quad [1]$$

The total calculated mass losses due to both reactants on the left side of Reaction [1] were calculated and the results are presented in Figure 5. Obviously, the carbothermic reduction of Na_2O from the slag can be considered as the main mechanism for Na_2O reduction with regard to mass balance results. The autoignition of the condensed material in the furnace can now be explained and obviously it is related to the re-oxidation of fine metallic Na particles, which are condensed from the gas phase. These Na particles are very fine due to the formation from the gas phase and their very high surface area causes observing their autoignition at room temperature, which is much lower than the reported autoignition temperature of Na as 393 K to 398 K (120 °C to 125 °C).[14]

In addition to the Reaction [1] at the slag/crucible contact area, limited amount of Na_2O is reduced at the slag/silicon interfacial area through the silicothermic reduction of Na_2O which causes small amount of Na transport to the metal:

$$Si + 2(Na_2O) = 2[Na] + (SiO_2). \quad [2]$$

The changes of Na concentration in the silicon and slag (Figure 3) show that Na mass transport to the gas phase at silicon-gas interfacial area is taking place simultaneously. Regarding the total Na in the system,

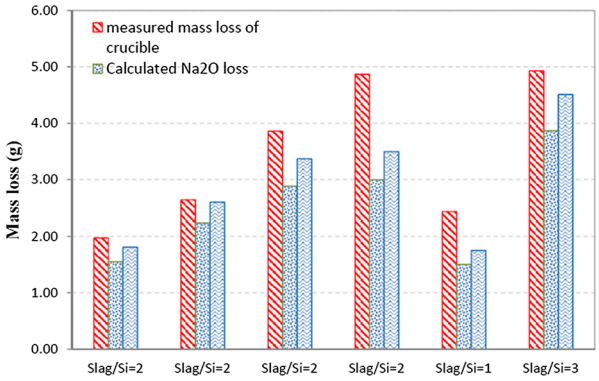

Fig. 5—Measured total mass losses, the calculated mass losses due to Na_2O loss, and mass loss through chemical Reaction [8].

small amount of Na is transferred to the silicon phase through Reaction [2] and therefore the Na loss share through evaporation of the dissolved Na in silicon is very small. The rest of the mass loss in the system in addition to Reaction [1] can be due to the graphite material volatilization or oxidation through any CO_2 gas produced in the system. The evaporation of Ca at silicon-gas interface and SiO formation at slag/crucible wall can potentially occur with small mass losses. In addition to the Reactions [1] and [2], the main other chemical reactions that can explain the results are shown in Figure 3 and can be written as:

$$Si + 2(CaO) = 2[Ca] + (SiO_2), \quad [3]$$

$$[Al] + (SiO_2) = (Al_2O_3) + Si. \quad [4]$$

Chemical Reaction [4] is thermodynamically favorable with regard to the higher oxidation potential of Al compared to Si, and Al concentration changes in silicon (Figure 3) show that Reaction [4] is fast from kinetic point of view. Reactions [2] and [3] cause limited mass transport of Na and Ca into the melt and this mass transport takes place with a high rate so that a concentration peak of these elements in silicon is observed in experiments with short refining times (Figure 3). The concentration of both Ca and Na is decreased after reaching a maximum. The changes of Na and Ca concentrations can be related to the Reactions [2] and [3] and the evaporation Reactions [5] and [6]:

$$[Na] = Na(g), \quad [5]$$

$$[Ca] = Ca(g). \quad [6]$$

From kinetic point of view, the evaporation of Na is more favorable than that of Ca due to higher activity coefficient of Na in Si than that of Ca and much higher vapor pressure of Na than that of Ca at a given temperature. The activity coefficients of Na and Ca at the silicon melting point are 0.466 and 0.003, respectively.[15] The faster Na evaporation may be a reason of observing much lower Na concentrations than Ca in silicon melt. The mass transport of Na and Ca is dependent on the slag/silicon ratio as seen in Figure 3. For a given reaction time, the Na concentration in the silicon melt is higher for higher slag/silicon ratio. This is due to the higher amount of Na_2O in the co-existing slag phase with slower Na_2O loss (Figure 3). In contrast, lower Ca concentration is seen for higher slag/silicon ratio. Since, there is a lot of Ca in the slag phase in all reaction times and the slag is in good contact with silicon melt, the concentration decreases for Ca after reaching the maximum cannot be due to evaporation. Hence, the Ca concentration changes in silicon after reaching a maximum are due to Ca return to the slag phase (Reaction [3] in backward) due to the Na_2O depletion from the slag phase and not Reaction [6]. It is worth mentioning that the equilibrium Ca concentrations in silicon in contact with 50 pctCaO-50 pctSiO_2 slags can be typically in the range from 800 to 1200 ppmw.[5] This return of Ca to the slag phase is required with regard to the slag structure and for energy minimization; Ca^{2+} cations are substituted Na^{+} cations to make non-bridging oxygen in the slag structure.

B. *Boron Removal*

The B concentration changes in silicon and slag phases (Figure 3) show that B is rapidly transported to the slag and its concentration is leveled off in both phases. Regarding B concentrations and considering slag mass changes, the amount of B in the silicon and slag can be calculated. The B removal degree from silicon can be further calculated:

$$\text{pct}B\,\text{removal} = \frac{C^{i}_{B,Si} - C^{t}_{B,Si}}{C^{i}_{B,Si}} \times 100, \quad [7]$$

where $C^{i}_{B,Si}$ and $C^{t}_{B,Si}$ are the concentrations of B in silicon at initial and arbitrary time t, respectively. The calculated results in Figure 6 illustrate that the rate of B removal from silicon by CaO-Na_2O-SiO_2 slag is high; more than 75, 81, and 90 pct removal degrees are observed when slag/silicon ratios are 1, 2, and 3, respectively. It goes without saying that Na_2O component in the system plays an important role and when higher amount of slag is used, there is more amount of Na_2O to react with the dissolved B in silicon:

$$3(Na_2O) + 2[B] = (B_2O_3) + 6[Na]. \quad [8]$$

The other reactions which can occur in the system are B removal by the other slag components according to the following reactions:

$$3(CaO) + 2[B] = (B_2O_3) + 3[Ca], \quad [9]$$

$$3/2(SiO_2) + 2[B] = (B_2O_3) + 3/2[Si]. \quad [10]$$

The thermodynamic activities of both CaO and SiO_2 in the slag phase are not significantly changed during refining due to the small concentration changes of them in the slag when Na_2O is reduced. Hence, observing

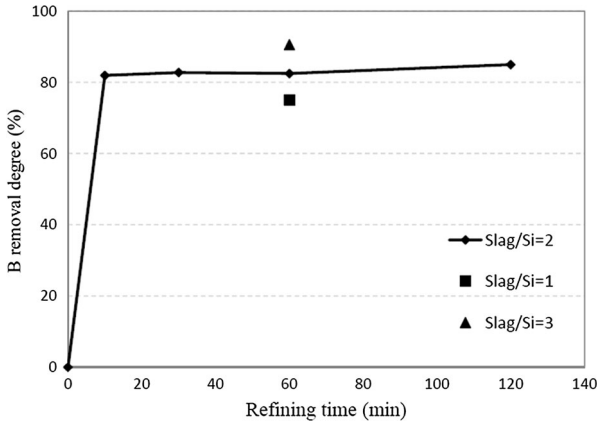

Fig. 6—Degree of B removal from silicon for the slag refining experiments.

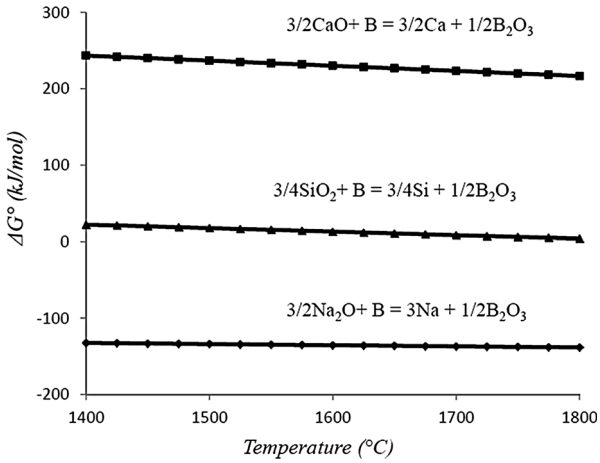

Fig. 7—The changes of the Gibbs free energy of oxidation of one mol B through Reactions [8] to [10].

better B removal for higher slag/metal ratios is not due to B oxidation by Reactions [9] and [10], and Reaction [8] may be the dominant reaction. It is worth noting that Al_2O_3 in the slag does not react with the dissolved B in silicon due to its very low concentration (25 to 50 ppm) and its high affinity in the slag which causes very low chemical activity. The presented data in Figure 3 about the Al concentration changes show clearly that Al is mainly distributed to the slag phase and there is no Al return from the slag to the silicon melt. This means that Al_2O_3 does not react with the dissolved B and even with the other melt components (Si and Ca). Figure 7 shows the calculated relationship between the changes in the standard Gibbs energy of formation of chemical Reactions [8] to [10] using HSC Chemistry 7.1 software. Although Figure 7 shows that B oxidation by Na_2O is the most favorable and oxidation by CaO is the lowest possible reaction, the Gibb energy of these reactions under non-standard conditions can be different due to the lower chemical activities than unity. In order to evaluate the competitiveness of Reactions [8] to [10] under real process conditions, we study here the changes

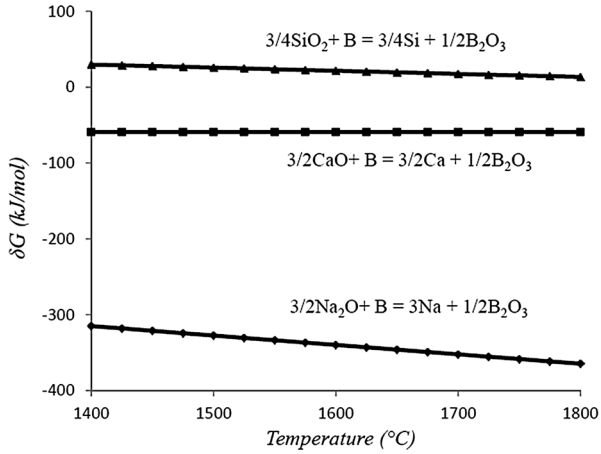

Fig. 8—The changes of δG_8, δG_9, and δG_{10} for B oxidation through Reactions [8] to [10].

in δG values, which are defined as below for the above reactions:

$$\delta G_8 = \Delta G_8 - RT\ln\left(\frac{a_{B_2O_3}}{a_B^2}\right) = \Delta G_8^\circ + RT\ln\left(\frac{a_{Na}^6}{a_{Na_2O}^3}\right), \quad [11]$$

$$\delta G_9 = \Delta G_9 - RT\ln\left(\frac{a_{B_2O_3}}{a_B^2}\right) = \Delta G_9^\circ + RT\ln\left(\frac{a_{Ca}^3}{a_{CaO}^3}\right), \quad [12]$$

$$\delta G_{10} = \Delta G_{10} - RT\ln\left(\frac{a_{B_2O_3}}{a_B^2}\right) = \Delta G_{10}^\circ + RT\ln\left(\frac{a_{Si}^{3/2}}{a_{SiO_2}^{3/2}}\right), \quad [13]$$

where ΔG_i is the Gibbs energy change of reaction (i). Since, we do not have thermodynamic data about the activity of B_2O_3 in the slag, studying the changes of δG values than ΔG values may be more reliable, since the same expression is subtracted from ΔG for all the reactions. Figure 8 shows the calculated δG values for the above three reactions between 1673 K and 2073 K (1400 °C and 1800 °C). For calculations, the activity data for CaO-SiO_2 and Na_2O-CaO-SiO_2 slag systems were considered in low Na_2O concentrations and below 5 wt pct Na_2O.[16] Moreover, the required activities for Ca and Na were determined for their highest observed concentrations shown in Figure 3 and by considering the previously determined activity coefficients of the dilute solutions of Ca and Na in silicon.[2,17] Figure 8 shows that the chemical Reaction [8] is the dominant reaction compared to Reactions [9] and [10] under non-standard conditions. This figure indicates also that B oxidation by CaO is more favorable than by SiO_2, which is completely different with the Reactions [9] an [10] under standard conditions in Figure 7.

Boron mass balance in the system shows that a part of B is gasified during refining. The B gasification degree

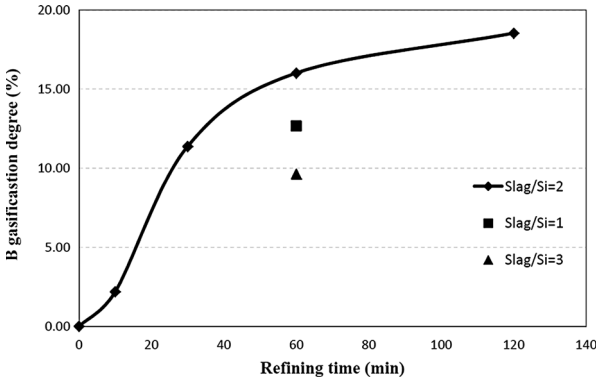

Fig. 9—Degree of B gasification in the refining experiments.

for all the experiments was calculated with regard to the concentrations of B in silicon and slag phases before and after refining. The illustrated results in Figure 9 show that B gasification is initially fast and then its rate is decreased. The B mass transport to the gas phase is due to the formation of sodium metaborate ($Na_2B_2O_4$) in the slag according to the following reaction:

$$(Na_2O \cdot B_2O_3) = Na_2B_2O_4(g). \qquad [14]$$

The vapor pressure of $Na_2B_2O_4$ is significantly higher than B_2O_3 and the B gasification is due to its formation and evaporation at slag-gas interfacial area.[2] Hence, the B gasification is in connection with the concentration of Na_2O in the slag and therefore the rate of the carbothermic reduction of Na_2O from the slag. As long as there is Na_2O in the slag phase, B gasification through Reaction [14] may take place and it is the reason of continuous B loss (Figure 9), while the B concentration in the slag is almost constant (Figure 3). Observing lower B gasification degree for slag/metal = 1 than that for slag/metal = 2 within the same time can be due to the less amount of Na_2O in exposure to the silicon. However, observing lower B gasification degree for the slag/metal = 3 is hard to be explained. An explanation is that the kinetics of B transport to the gas phase is potentially dependent on the mass transport of B_2O_3 from slag–silicon interface to the slag–gas interface.

C. *Boron Distribution*

The analysis data in Figure 3 can be considered to evaluate the distribution of B between the slag and silicon phases. The very low Na_2O concentrations in slag in long refining time cause very slow $Na_2B_2O_4$ evaporation at the slag-gas interface and therefore negligible further B loss through sodium metaborate evaporation. Therefore, the distribution of B between the slag and silicon may be close to equilibrium, if the B removal from the system (slag + silicon) is controlled by $Na_2B_2O_4$ evaporation at the slag surface. This is confirmed with regard to the concentration of B in both silicon and slag in experiments 1 to 4 so that B concentration is leveled off in long reaction times. As mentioned before, the distribution of B between slag and silicon is evaluated by L_B, which is as follows:

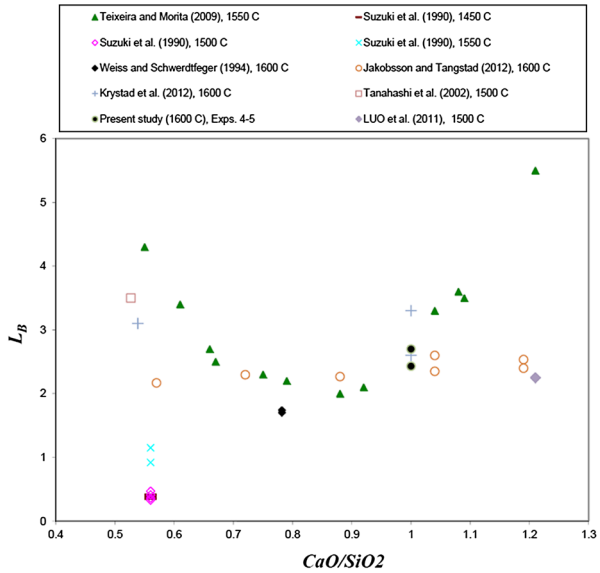

Fig. 10—Distribution of B between the slag and silicon (L_B) for experiments 4 and 5 in comparison with the literature data.

$$L_B = \frac{(\text{Pct B})_{\text{slag}}}{[\text{Pct B}]_{\text{silicon}}}. \qquad [15]$$

The L_B values for experiments 4 and 5 in which the Na_2O concentration is very low were determined and the results are shown in Figure 10, in comparison with the literature data for B distribution between silicon and $CaO\text{-}SiO_2$ slags. The point for the Tanahashi *et al.*[10] is for a slag containing 0.2 wt pct Na_2O. Although the literature data for L_B are quite scattered for the $CaO\text{-}SiO_2$ slag system, the obtained results in the present study are in relatively good agreement with the other works for CaO/SiO_2 ratio around unity.[5,8,9] The thermodynamic equilibrium data presented in Figure 8 have been mainly established through long interaction times, while relatively close ratios of (pctB)/[pctB] to the equilibrium L_B values are obtained in much shorter reaction times in the present study. This may indicate that the kinetics of B removal from the slag is significantly affected by the Na_2O and Reaction [8] takes place rapidly at the slag-metal interface. The (pctB)/[pctB] ratio in Exp. 6 of 3.3 is higher than that observed in the other experiments and this may be due to the effect of Na_2O in the system. This is in agreement with literature, where higher borate capacities for the $Na_2O\text{-}CaO\text{-}SiO_2$ slags than $CaO\text{-}SiO_2$ slags have been observed.[6,10]

D. *Kinetics of B removal from silicon*

Based on the kinetics principles and considering a first-order reaction for the B oxidation at slag/metal interface, the rate constant can be calculated as:

$$k_{B,\text{app}} = \frac{\ln\left[\left(C^{i}_{B,Si} - C^{eq}_{B,Si}\right)/\left(C^{t}_{B,Si} - C^{eq}_{B,Si}\right)\right]}{(A_{\text{slag-Si}}/V_{Si})t}, \qquad [16]$$

where $A_{slag–Si}$ is the slag–silicon interfacial area and V_{Si} is the molten silicon volume. Estimating these values based on the properties of molten silicon[18] and the melt geometry described above, the apparent rate constant $k_{B,app}$ for experiment 1 was calculated as $k_{B,app} = 5.8 \times 10^{-5}$ m/s. For the calculations, $L_B = 2.4$ was considered (Figure 10) and it yields the equilibrium concentration of B in silicon as $C^{teq}_{B,Si} = 4.5$ppmw, considering the final B concentration in the slag around 10.8 ppmw (Figure 3). Similar calculation for longer refining times may provide large errors in calculating the rate constant due to the large extent of B removal down to around slag–silicon equilibrium in short times. The calculated rate constant here is much larger than the determined rate constants for B removal by $CaO-SiO_2$ slags by Krystad *et al.*[9] as 1.7×10^{-6} m/s for $CaO/SiO_2 = 1$, and 3.5×10^{-6} m/s for $CaO/SiO_2 = 0.54$ at 1873 K (1600 °C). Nishimoto and Morita[19] also calculated rate constant as 1.4×10^{-6} m/s for $CaO/SiO_2 = 1.2$ using this binary slag at the same temperature. The much higher rate constant obtained by $Na_2O-CaO-SiO_2$ slags in this study is attributed to B removal mechanism, which is through Reaction [8]. When Na_2O does not exist, the main reaction for B removal is Reaction [10], which is less favorable than Reaction [8] from thermodynamics point of view.[2]

The other parameter which may have affected the kinetics of B removal in the present study is the use of induction furnace, while in the above mentioned works[3–10] the refining experiments were carried out in resistance furnaces. Since the slag is not conductive, the electromagnetic forces in induction furnace may not significantly affect the mass transport in the slag phase. In contrast, molten silicon is a conductive matter and therefore the electromagnetic forces may enhance the mass transport of B in the metal phase through extensive inductive stirring. Based on the previous outlined method for determining the diffusivity of elements in liquid silicon,[15] the diffusivity of B in molten silicon at 1873 K (1600 °C) was calculated as 1.49×10^{-8} m^2/s. Considering the developed theory by Machlin for mass transport in inductively stirred melts,[20] this yields a mass transfer coefficient of B in a melt boundary layer (adjacent to the slag-metal interface) in liquid silicon as $k_{B,melt} = 3.7 \times 10^{-4}$ m/s. This higher mass transfer coefficient of B in the melt boundary layer than the determined total mass transfer coefficient (5.8×10^{-5} m/s), which is around six times larger, may indicate that the kinetics of B removal is controlled by the chemical Reaction [8] at the slag-metal interface, or mass transport in the slag phase, or combination of the two stages.

E. *Comparison of $Na_2O-CaO-SiO_2$ Slags with Na_2O-SiO_2 Slags*

Both the present work results in using the ternary 5 pctNa_2O-47.5 pctCaO-47.5 pctSiO_2 slag and the former study[2] in using Na_2O-SiO_2 slags indicate high potential of both slags in B elimination from silicon. In both cases, Na_2O is removed from the slag phase and a small portion of it in the form of $Na_2B_2O_4$ gas which causes B loss from the system. However, when Na_2O-SiO_2 slags were used, the majority of the B was removed to the gas phase. Although higher amounts of Na_2O were used, the ratio of B in slag over that in the silicon, (pctB)/[pctB], was low. For instance, when 50 pctNa_2O-50 pctSiO_2 slag was used this ratio was as (pctB)/[pctB] = 1. Whereas when the ternary slag is used, we see (pctB)/[pctB] ratio greater than 2.4. These may indicate that boron oxide in the Na_2O-pctCaO-pctSiO_2 slags is more stable than Na_2O-SiO_2 slags so that its evaporation through sodium metaborate formation occurs with slower rate. Hence, the kinetics of B removal from the slag is mainly controlled by the rate of the evaporation of chemical reaction of $Na_2B_2O_4$. An important message here is that boron oxide is better accumulated in the structure of $CaO-SiO_2$ slags than Na_2O-SiO_2 slags. In fact, the L_B value, which is depending on slag basicity, and $Na_2B_2O_4$ gas formation, which is depending on the slag chemistry and temperature, are both affecting the kinetics of B removal from silicon. Hence, proper slag composition, maintaining larger L_B value, and higher temperature may provide faster B removal rate. Addition of Na_2O to the slags that show large L_B values such as $CaO-SiO_2-CaF_2$ slags[21] may be interesting to be studied.

V. CONCLUSIONS

The removal of B from silicon through refining by 5 pctNa_2O-47.5 pctCaO-47.5 pctSiO_2 slag at 1600 °C was studied and the following conclusions were made:

1. Rapid mass transport of B, Na, Ca, and Al occurs through the interaction of slag and silicon. The majority of B and Al are transported to the slag, while small amounts of Na and Ca are transported from the slag to silicon.
2. The transported B to the slag is partially gasified through evaporation of sodium metaborate at slag-gas interface and B gasification is in a larger extent for higher slag/silicon ratios. The kinetics of this chemical reaction is rate limiting for B removal from the slag phase.
3. The kinetics of B removal from silicon by Na_2O-containing slags is controlled by the chemical oxidation reaction of B by Na_2O at slag–silicon interface and mass transport of the boron oxide in the slag phase.
4. A high apparent rate constant for B removal from silicon as $k_{B,app} = 5.8 \times 10^{-5}$ m/s was determined, which is higher than literature data on slag refining of silicon.
5. The ratio of B concentration in slag over that in silicon is close to the equilibrium L_B value for $CaO-SiO_2$ slag ($CaO/SiO_2 = 1$). L_B values as 2.4 and 2.6 were obtained for very low Na_2O concentrations in the slag.
6. It is proposed that boron oxide (B_2O_3) is better embedded in the structure of $CaO-SiO_2$ slags than Na_2O-containing slags.

ACKNOWLEDGMENTS

The authors acknowledge the funding provided through the BASIC project (191285/V30) by the Norwegian Research Council. The authors acknowledge silicon material support from ELKEM AS.

REFERENCES

1. J. Safarian, G. Tranell, and M. Tangstad: *Energy Proc.*, 2012, vol. 20, pp. 88–97.
2. J. Safarian, G. Tranell, and M. Tangstad: *Metall. Mater. Trans. B*, 2013, vol. 44B, pp. 571–83.
3. K. Suzuki, T. Sugiyama, K. Takano, and N. Sano: *J. Jpn. Inst. Met.*, 1990, vol. 54, pp. 168–72.
4. T. Weiss and K. Schwerdtfeger: *Metall. Mater. Trans. B*, 1994, vol. 25B, pp. 497–504.
5. L.A.V. Teixeira, Y. Tokuda, T. Yoko, and K. Morita: *ISIJ Int.*, 2009, vol. 49, pp. 777–82.
6. L.A.V. Teixeira, Y. Tokuda, T. Yoko, and K. Morita: *ISIJ Int.*, 2009, vol. 49, pp. 783–87.
7. D.W. Luo, N. Liu, Y.P. Lu, G.L. Zhang, and T.J. Li: *Trans. Nonferrous Met. Soc. China*, 2011, vol. 21, pp. 1178–84.
8. L.K. Jakobsson and M. Tangstad: *International Smelting Technology Symposium (Incorporating the 6th Advances in Sulfide Smelting Symposium)*, J.P. Downey, T.P. Battle, J.F. White, eds., TMS 2012, Orlando, FL, pp. 179–84.
9. E. Krystad, J. Kline, M. Tangstad, and G. Tranell: *Ninth International Conference on Molten Slags, Fluxes and Salts (MOLTEN12)*, Beijing, China, 2012.
10. M. Tanahashi, Y. Shinpo, T. Fujisawa, and C. Yamauchi: *J. Min. Mat. Proc. Inst. Jpn.*, 2002, vol. 118, pp. 497–505.
11. J.R. Davis, A. Rohatgi, R.H. Hopkins, P.D. Blais, P. Rai-Choudhury, J.R. Mccormick, and H.C. Mollenkopf: *IEEE Trans. Elect. Dev.*, 1980, vol. ED-27, pp. 677–687.
12. P. Galler, A. Raab, S. Freitag, K. Blandhol, and J. Feldmann: *Silicon for the Chemical and Solar Industry XII*, June 2014, Trondheim, Norway, pp. 101–11.
13. M. Kadkhodabeigi, J. Safarian, H. Tveit, M. Tangstad, and S.T. Johansen: *Trans. Nonferrous Met. Soc. China*, 2012, vol. 22, pp. 2813–21.
14. Chemical Hazard Response Information System: United States Coast Guard, COMDTINST M16465.12C, 1999.
15. J. Safarian and M. Tangstad: *Metall. Mater. Trans B*, 2012, vol. 43B, pp. 1427–45.
16. M. Allibert, R. Para, C. Saint-Jours, and M. Tmar: *Slag Atlas*, Verlag Stahleisen GmbH, Dusseldorf, 1995, pp. 225–45.
17. J. Safarian, L. Kolbeinsen, and M. Tangstad: *Metall. Mater. Trans. B*, 2011, vol. 42B, pp. 852–74.
18. J. Safarian and M. Tangstad: *High Temp. Mater. Proc.*, 2012, vol. 31, pp. 73–81.
19. H. Nishimoto and K. Morita: *TMS Suppl. Proc.*, 2011, vol. 1, pp. 701–08.
20. E.S. Machlin: *Trans. TMS-AIME*, 1960, vol. 218, pp. 314–26.
21. J. Cai, J. Li, W. Chen, C. Chen, and X. Luo: *Trans. Nonferrous Met. Soc. China*, 2011, vol. 21, pp. 1402–06.